Available online at www.sciencedirect.com
SCIENCE DIRECT®
International Journal of Solids and Structures 43 (2006) 4704–4719
INTERNATIONAL JOURNAL OF SOLIDS and STRUCTURES
www.elsevier.com/locate/ijsolstr

Imperfection sensitivity analysis of hill-top branching with many symmetric bifurcation points

Makoto Ohsaki [a,*], Kiyohiro Ikeda [b,1]

[a] Department of Architecture and Architectural Engineering, Kyoto University, Nishikyo, Kyoto-daigaku Katsura, Kyoto 615-8540, Japan
[b] Department of Civil Engineering, Tohoku University, Aoba, Sendai 980-8579, Japan

Received 29 March 2005
Available online 8 August 2005

Abstract

Imperfection sensitivity properties are derived for finite dimensional elastic conservative systems exhibiting hill-top branching at which arbitrary many bifurcation points coincide with a limit point. The critical load at a hill-top branching point is demonstrated to be insensitive to initial imperfections when all the bifurcation points are individually symmetric. Therefore, it is not dangerous to design a frame or truss so that many members buckle simultaneously at the limit point, although the notion of the danger of optimization by compound bifurcation is widespread.

Keywords: Coincident buckling; Hill-top branching; Imperfection sensitivity; Member buckling; Symmetric bifurcation

1. Introduction

The simultaneous buckling was studied in association with optimization. The principle of simultaneous mode design states, "A given form will be optimum if all failure modes which can possibly intersect occur simultaneously (Spunt, 1971)". The danger of naive optimization without due regard to imperfection sensitivity and the erosion of optimization by compound branching were suggested (Thompson and Supple, 1973). Various kinds of structures were found highly imperfection-sensitive when two or more bifurcation points are nearly or strictly coincident, and are subjected to interaction of buckling modes, such as local and global modes (Hutchinson and Amazigo, 1967; Koiter and Kuiken, 1971; Thompson and Lewis,

* Corresponding author. Tel.: +81 75 383 2901; fax: +81 75 383 2972.
E-mail addresses: ohsaki@archi.kyoto-u.ac.jp (M. Ohsaki), ikeda@civil.tohoku.ac.jp (K. Ikeda).
[1] Tel.: +81 22 795 7416; fax: +81 22 795 7418.

0020-7683/$ - see front matter © 2005 Elsevier Ltd. All rights reserved.
doi:10.1016/j.ijsolstr.2005.06.036

1972; Tvergaard, 1973). Thompson and Hunt (1974) suggested extreme enhancement of imperfection sensitivity due to modal interaction as a result of optimization; imperfection sensitivity of coincident critical points was studied thereafter (Thompson and Hunt, 1984; Hunt, 1986).

Yet such severe enhancement of imperfection sensitivity is absent for another kind of coincident critical points. A nearly coincident pair of a bifurcation point and a limit point of loading parameter was found in (a) numerical simulation of a long tensile steel specimen undergoing plastic instability (Needleman, 1972), and (b) mechanical instability of stressed atomic crystal lattices (Thompson and Schorrock, 1975). Such a pair of points was approximated by a hill-top branching (bifurcation) point, at which the pair of points coincide strictly. This hill-top point was shown to enjoy locally piecewise linear imperfection sensitivity (Thompson and Schorrock, 1975; Thompson, 1982; Ikeda et al., 2002; Okazawa et al., 2002), which is less severe than the two-thirds power-law for a simple pitchfork bifurcation point. A piecewise linear relationship was also observed for other hill-top branching points that occur as the coincidence of

(i) an asymmetric bifurcation point and a limit point (Ohsaki, 2003), and
(ii) a limit point and a double bifurcation point studied by a group-theoretic approach (Ikeda et al., 2005).

Ohsaki (2000) optimized shallow trusses under constraints on nonlinear buckling and found that the optimum solution usually has a hill-top branching point, which is not sensitive to imperfections. Thus the optimization for nonlinear buckling does not always produce a dangerous structure.

It is noteworthy that, for a pin-jointed truss, member buckling can occur almost independently from global buckling (Peek and Triantafyllidis, 1992). Therefore, it is possible to create a hill-top branching point at which arbitrary many symmetric bifurcation points can exist at a limit point; i.e. many members buckle simultaneously with global buckling.

The basic framework to deal with coincident critical points can be found in the static perturbation method (Supple, 1967, 1968; Thompson and Hunt, 1973, 1984; Godoy, 1999); in this framework, compound bifurcations were studied in detail (Hunt, 1981). Critical points can be classified by investigating the linear, quadratic, cubic, quartic, etc., terms of the total potential energy (Thompson and Hunt, 1973). The interaction between bifurcation modes is classified into third-order and fourth-order interactions; the third-order interaction exists if one of the bifurcation modes is asymmetric. The maximum load of an imperfect symmetric system is reduced if the fourth-order cross-term is negative (Thompson and Hunt, 1984).

In this paper, imperfection sensitivity of a hill-top branching point with many symmetric bifurcation points is investigated. This point is actually created for a pin-jointed truss with simultaneously buckling members. The bifurcation modes are individually symmetric among themselves, but some modes have infinitesimally small third-order interaction. The symmetry conditions with respect to bifurcation modes and limit-point-type mode are relaxed by ignoring such interaction to account for practical situation of member buckling at the limit point.

2. Illustrative example of a hill-top branching

We start with a simple illustrative example: a two-bar truss as shown in Fig. 1, where $H = 100$ mm and $L = 1000$ mm. The members are connected to the nodes by pin joints. Each member is divided into four beam elements to implement member buckling. Green's strain is used for representing geometrically nonlinear strain–displacement relation. In the following, the units of length and force are mm and kN, respectively.

Maple 9, a symbolic computation software, is used for the differentiation of the total potential energy with respect to displacements, imperfection parameters, etc. The equilibrium paths are traced by

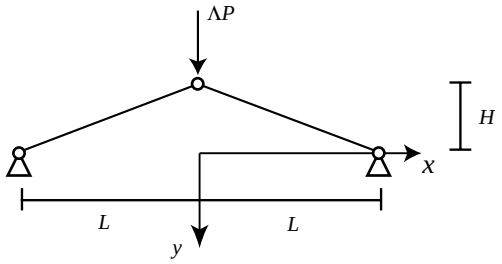

Fig. 1. A two-bar pin-jointed truss.

a displacement increment method with sufficiently small increments, and it has been confirmed that unbalanced loads at every incremental step are very small.

Let I and A, respectively, denote the second moment of area and the cross-sectional area of the members which have a $D \times D$ solid square cross-section; i.e. $I = D^4/12 = A^2/12$. The elastic modulus is denoted by E. The vertical load is defined by a unit load P and load factor Λ as ΛP, and Λ is increased to find the critical load factor Λ^c where the lowest eigenvalue of the tangent stiffness matrix vanishes. Fig. 2 shows the variation of the critical load ratio $\Lambda^c P/(EA)$ plotted against A. For a large value of A, the critical point is governed by a limit point. On the other hand, if A is small, member buckling occurs before reaching the limit point.

Consider an optimization problem of maximizing $\Lambda^c P/(EA)$ that is conceived as the critical load for the unit cost. It is seen from Fig. 2 that $\Lambda^c P/(EA)$ increases as A is increased from 0. At $A = A^* \simeq 3984.0$, bifurcation points exist at the limit point, which is called a hill-top branching point. For $A \geqslant A^*$, $P^c/(EA)$ is constant; accordingly, the structure with $A = A^*$ can be regarded as the optimal solution that achieves the maximum $\Lambda^c P/(EA)$ with the smallest A. As we have seen, structural optimization entails hill-top branching.

Fig. 3 shows the relation between ΛP and the vertical displacement v at the center node for $A = 3000.0$ that has a double bifurcation point before reaching a limit point, where $E = 1$ for simplicity. The eigenmodes $\hat{\boldsymbol{p}}_1$ and $\hat{\boldsymbol{p}}_2$ for zero eigenvalues at the double bifurcation point are shown in Fig. 4. Notice that only member buckling occurs in both $\hat{\boldsymbol{p}}_1$ and $\hat{\boldsymbol{p}}_2$. Let $\boldsymbol{U}^c$ denote the nodal displacement vector at the double bifurcation point. Deformation in the vicinity of $\boldsymbol{U}^c$ is defined as

$$\boldsymbol{U} = \boldsymbol{U}^c + q_1\hat{\boldsymbol{p}}_1 + q_2\hat{\boldsymbol{p}}_2 \tag{1}$$

where q_1 and q_2 are called generalized coordinates. The contour map of the total potential energy V scaled as $10{,}000(V + 12.2896)$ is plotted in Fig. 5 with respect to q_1 and q_2. Since $\hat{\boldsymbol{p}}_1$ is antisymmetric with respect

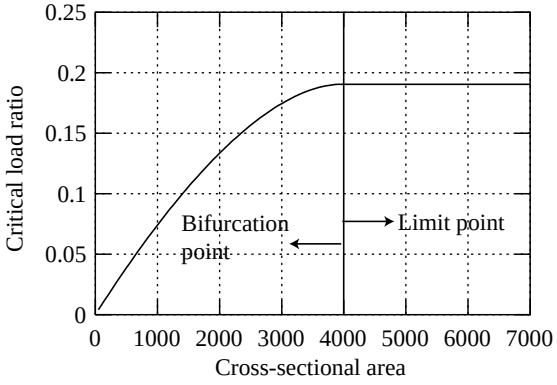

Fig. 2. Relation between the cross-sectional area and critical load ratio of the two-bar truss.

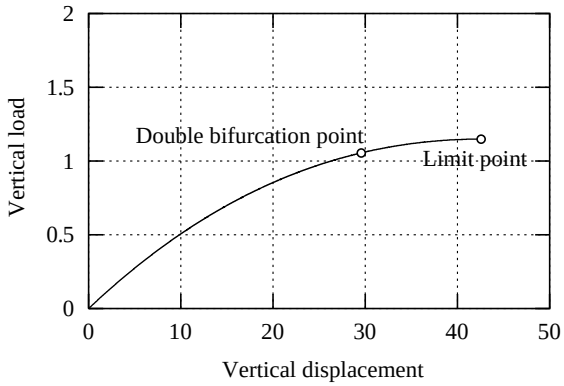

Fig. 3. Relation between vertical displacement and load for $A = 3000.0$.

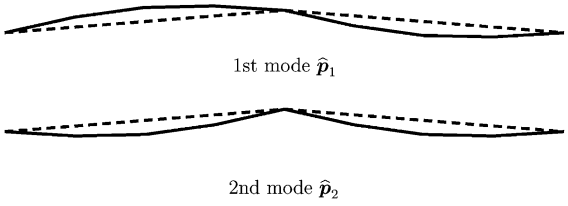

Fig. 4. Eigenmodes corresponding to the two zero eigenvalues at the double bifurcation point for $A = 3000.0$.

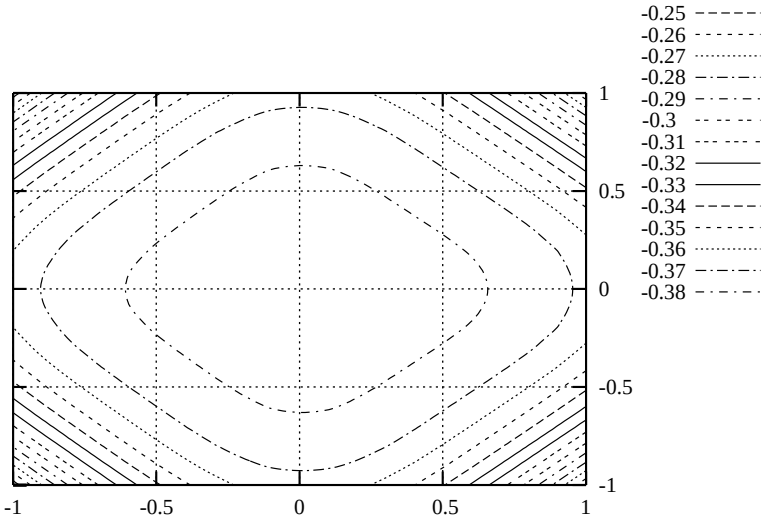

Fig. 5. Contour map of the scaled total potential energy $10{,}000(V + 12.2896)$ at the double bifurcation point for $A = 3000.0$.

to the vertical reflection axis of the truss, V is a symmetric (even) function of q_1. Although the deformations defined by $\boldsymbol{U}^{\mathrm{c}} + q_2\hat{\boldsymbol{p}}_2$ and $\boldsymbol{U}^{\mathrm{c}} - q_2\hat{\boldsymbol{p}}_2$ have different properties, V is almost symmetric with respect to q_2 as can be seen from Fig. 5, because only member buckling occurs in $\hat{\boldsymbol{p}}_2$ and is not influential on nodal displacements.

Fig. 6 shows the relation between ΛP and the vertical displacement v at the center node for $A = A^*$. It is confirmed from Fig. 6 that a limit point is reached as v is increased. The eigenvalues of the tangent stiffness matrix are plotted in Fig. 7. It should be noted that the three lowest eigenvalues do not coincide before reaching the hill-top point, where they simultaneously vanish. The eigenmodes corresponding to the three eigenvalues are as shown in Fig. 8. The eigenmode $\hat{\boldsymbol{p}}_2$ corresponds to a symmetric bifurcation due to member buckling without displacement at the center node, and $\hat{\boldsymbol{p}}_1$ and $\hat{\boldsymbol{p}}_3$ are the mixture of limit-point mode and bifurcation mode due to member buckling. Thus the coincidence of a limit point and bifurcation points incurs the mixing of eigenmodes.

Since any linear combination of critical modes at a coincident critical point is also a critical mode, it is possible to extract the limit point mode and the bifurcation mode due to member buckling from the critical modes mixed in this manner. From the general theory of elastic stability (Thompson and Hunt, 1973), the limit-point mode can be obtained from the incremental displacement along the fundamental equilibrium path at the limit point, which turns out to be the third mode $\boldsymbol{p}_3$ in Fig. 9. The bifurcation mode $\boldsymbol{p}_1$ in

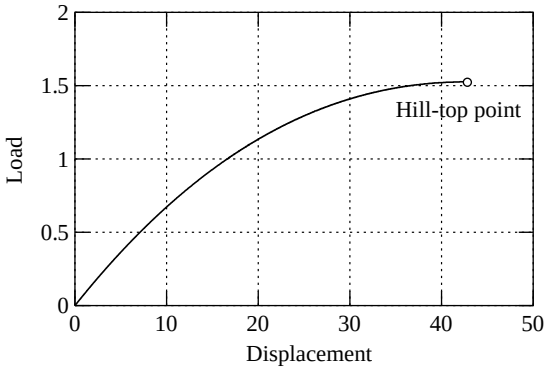

Fig. 6. Relation between vertical displacement and load for $A = A^*$.

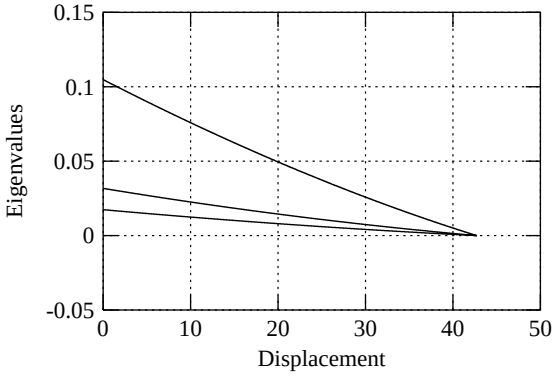

Fig. 7. Relation between vertical displacement and eigenvalues for $A = A^*$.

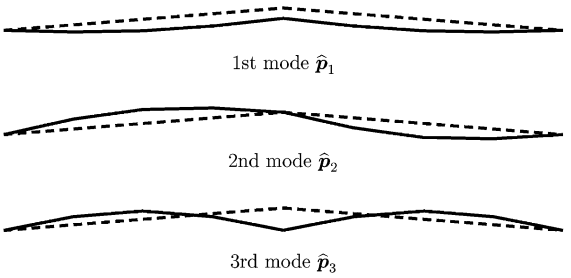

Fig. 8. Orthogonal eigenmodes corresponding to the three zero eigenvalues at the hill-top point.

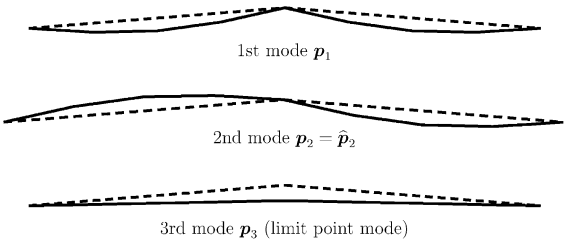

Fig. 9. Nonorthogonal eigenmodes corresponding to the three zero eigenvalues at the hill-top point.

Fig. 9 is obtained as a pertinent linear combination of $\hat{\boldsymbol{p}}_1$ and $\hat{\boldsymbol{p}}_3$ in Fig. 8 so that the vertical displacement of the center node vanishes.

The third-order differential coefficients V_{ijk} of the total potential energy in the directions of modes i, j, k (=1, 2, 3) in Fig. 9 are obtained as

$$\begin{aligned}
&V_{111} = 2.8454 \times 10^{-10}, \quad V_{112} = 5.0485 \times 10^{-15}, \quad V_{113} = 7.8384 \times 10^{-5},\\
&V_{122} = -2.6232 \times 10^{-10}, \quad V_{123} = 1.2865 \times 10^{-11}, \quad V_{133} = 2.8728 \times 10^{-13},\\
&V_{222} = 2.6394 \times 10^{-15}, \quad V_{223} = 7.8385 \times 10^{-5}, \quad V_{233} = 1.2026 \times 10^{-12},\\
&V_{333} = 7.4097 \times 10^{-5}
\end{aligned} \tag{2}$$

Since the loaded center node moves in $\boldsymbol{p}_3$, and V_{333} has larger value than V_{111} and V_{222}, $\boldsymbol{p}_3$ can be confirmed to be a limit-point mode. $\boldsymbol{p}_2$ is a symmetric bifurcation mode, because it is antisymmetric with respect to y-axis. $\boldsymbol{p}_1$ is an almost symmetric (slightly asymmetric) mode, because V_{111} has a very small value, although the mode shape is not antisymmetric. The symmetricity may be further investigated by computing the fifth and higher differential coefficients of V. In the following sections, general formulations are presented for imperfection sensitivity for a hill-top branching point with arbitrary many symmetric bifurcation points.

3. Hill-top branching of the perfect system

We next consider a general case of finite dimensional geometrically nonlinear structure, of which the deformation is described by the nodal displacement vector $\boldsymbol{U} = (U_1, \ldots, U_n)$, where n is the number of degrees of freedom. We assume the existence of the total potential energy $\overline{V}(\boldsymbol{U}, \Lambda)$ that is a smooth function of $\boldsymbol{U}$ and loading parameter Λ.

Denote by $\boldsymbol{H}$ the Hessian of $\overline{V}$ with respect to $\boldsymbol{U}$, which is called tangent stiffness matrix. The eigenvalue problem of $\boldsymbol{H}$ is formulated as

$$\boldsymbol{H}\hat{\boldsymbol{p}}_i = e_i\hat{\boldsymbol{p}}_i \quad (i = 1, \ldots, n) \tag{3}$$

where e_i is the ith lowest eigenvalue ($e_i \leqslant e_{i+1}$), and $\hat{\boldsymbol{p}}_i$ is the associated eigenvector normalized by $\hat{\boldsymbol{p}}_i^{\mathrm{T}}\hat{\boldsymbol{p}}_i = 1$ ($i = 1, \ldots, n$), where $()^{\mathrm{T}}$ denotes the transpose of a vector.

Consider a case where $m-1$ bifurcation points exist at a limit point; i.e. the critical point is a hill-top branching point with m lowest eigenvalues vanishing simultaneously. To separate the bifurcation modes and the limit-point mode, the increment of $\boldsymbol{U}$ at the limit point along the fundamental equilibrium path is used for defining the limit point mode $\boldsymbol{p}_m$ as demonstrated in the previous section. The bifurcation modes $\boldsymbol{p}_i$ ($i = 1, \ldots, m-1$) are obtained by removing the component of $\boldsymbol{p}_m$ from $\hat{\boldsymbol{p}}_i$ as

$$\boldsymbol{p}_i = \hat{\boldsymbol{p}}_i + c_i\boldsymbol{p}_m \quad (i = 1, \ldots, m-1) \tag{4}$$

where the coefficient c_i is computed from

$$\boldsymbol{p}_m^{\mathrm{T}}(\hat{\boldsymbol{p}}_i + c_i\boldsymbol{p}_m) = 0 \quad (i = 1, \ldots, m-1) \tag{5}$$

The generalized coordinate q_j in the direction of $\boldsymbol{p}_j$ is defined by the transformation

$$\boldsymbol{U} = \boldsymbol{U}^{\mathrm{c}} + \sum_{j=1}^{n} q_j\boldsymbol{p}_j \tag{6}$$

where $\boldsymbol{U}^{\mathrm{c}}$ is the displacement vector at the critical point.

Denote by $q_1, \ldots, q_{m-1}$ the generalized coordinates in the direction of bifurcation modes measured from the hill-top point, and by q_m that in the direction of limit-point mode. Then $q_1, \ldots, q_m$ serve as active coordinates and $q_{m+1}, \ldots, q_n$ as passive coordinates. The increment of the loading parameter from the hill-top point is denoted by λ.

The total potential energy is defined as a function of $\boldsymbol{q} = (q_1, \ldots, q_n)$ and λ and is written as $V(\boldsymbol{q}, \lambda)$. Differentiation with respect to q_i is indicated by a subscript i. The equilibrium equations are written as

$$V_i = 0 \quad (i = 1, \ldots, n) \tag{7}$$

Since m lowest eigenvalues e_i ($i = 1, \ldots, m$) vanish at the hill-top point, the following relations hold:

$$V_{ij} = 0 \quad (i, j = 1, \ldots, m) \tag{8}$$

For the modes $\boldsymbol{p}_i$ ($i = m+1, \ldots, n$) higher than m, orthogonality conditions

$$\boldsymbol{p}_i^{\mathrm{T}}\boldsymbol{p}_j = 0 \quad (i, j = m+1, \ldots, n; i \neq j) \tag{9}$$

should be satisfied so that V_{ij} is diagonalized such that

$$V_{ij} = 0 \quad (i, j = m+1, \ldots, n; i \neq j) \tag{10}$$

$$V_{ij} = V_{ji} = 0 \quad (i = 1, \ldots, m; j = m+1, \ldots, n) \tag{11}$$

Note that the orthogonality among the eigenvectors $\boldsymbol{p}_i$ ($i = 1, \ldots, m$) need not be satisfied, because, for multiple eigenvalues, any linear combination of the eigenvectors is also an eigenvector.

From the conditions of limit point and bifurcation points,

$$V'_i = 0 \quad (i = 1, \ldots, m-1) \tag{12}$$

$$V'_m \neq 0 \tag{13}$$

are to be satisfied, where $()'$ indicates differentiation with respect to λ.

4. Imperfection sensitivity analysis at hill-top point

We move on to consider a critical point of an imperfect system. Let ε denote the imperfection parameter. The total potential energy of an imperfect system, which is a function of $n+2$ variables $\lambda, q_1, \ldots, q_n$ and ε, is written as $V(\boldsymbol{q}, \lambda, \varepsilon)$. Since n equilibrium equations (7) should be satisfied for $n+2$ variables, an equilibrium state is to be determined by specifying two variables; say, e.g., ε and λ.

Suppose without loss of generality that the imperfection is influential both on the bifurcation modes and the limit-point mode; i.e. q_1 and q_m are assumed to have nonzero values at a critical point of the imperfect system. Then q_1 and q_m can be taken as two independent parameters, and the following relations hold:

$$q_{1m} = q_{m1} = 0, \quad q_{11} = q_{mm} = 1 \tag{14}$$

where q_{ij} denote differentiation of q_i with respect to q_j.

Differentiating the ith equilibrium equation $V_i = 0$ in (7) with respect to q_s ($s = 1$ or m) leads to

$$\sum_{j=1}^{n} V_{ij} q_{js} + V'_i \lambda_s + \dot{V}_i \varepsilon_s = 0 \quad (i = 1, \ldots, n; s = 1 \text{ or } m) \tag{15}$$

where a dot denotes differentiation with respect to ε.

For $i = 1$ or m, incorporating (8), (10)–(12) into (15) results in

$$\lambda_s = \varepsilon_s = 0 \quad (s = 1 \text{ or } m) \tag{16}$$

For $i = m+1, \ldots, n$, incorporating (16) into (15) results in

$$q_{is} = 0 \quad (s = 1 \text{ or } m) \tag{17}$$

Therefore, the differential coefficients of the passive coordinates q_i ($i = m+1, \ldots, n$) vanish, and, in turn, the passive coordinates have lower order than the two active coordinates q_1 and q_m; i.e.

$$|q_i| \ll |q_s| \quad (i = m+1, \ldots, n; s = 1 \text{ or } m) \tag{18}$$

By further differentiating (15) with respect to q_t ($t = 1$ or m) and using (8), (10), (11), (16), and (17), we obtain

$$V_{ii} q_{ist} + \sum_{j=1}^{m} \sum_{k=1}^{m} V_{ijk} q_{js} q_{kt} + V'_i \lambda_{st} + \dot{V}_i \varepsilon_{st} = 0 \quad (s, t = 1, m; i = 1, \ldots, n) \tag{19}$$

Letting $(i, s, t) = (1, 1, m)$ in (19),

$$V_{11m} + \dot{V}_1 \varepsilon_{1m} = 0 \tag{20}$$

is obtained; i.e. $\varepsilon_{1m} \neq 0$ and ε has the quadratic order of the two active coordinates. Similarly, if we set $(i, s, t) = (m, m, m)$ in (19),

$$V_{mmm} + V'_m \lambda_{mm} = 0 \tag{21}$$

is obtained; i.e. $\lambda_{mm} \neq 0$ and λ also has the quadratic order. Finally, it is easily observed from (19) for $i > m$ that $q_{ist} \neq 0$ is satisfied; i.e. the passive coordinates are also quadratic function of the active coordinates. Note that these relations are satisfied if at least one bifurcation point exists at a limit point.

Hence, the following relations hold:

$$\begin{cases} |q_i| = \mathrm{O}(\varepsilon^{1/2}) & (i = 1, \ldots, m) \\ |q_i| = \mathrm{O}(\varepsilon) & (i = m+1, \ldots, n) \\ |\lambda| = \mathrm{O}(\varepsilon) \end{cases} \tag{22}$$

i.e. the load factor λ has the linear order of the imperfection parameter ε.

As the objective of this paper, quantitative imperfection sensitivity analysis is conducted by using the third-order systems along with the static perturbation procedure by Thompson (1982). In the following, all variables are evaluated at the hill-top point.

Assumptions on the derivatives of V employed are

- All $m-1$ bifurcation points are symmetric, and V is individually symmetric (Thompson and Hunt, 1984) up to the third-order terms in the subspace of the bifurcation modes; i.e.

$$V_{ijk} = 0 \quad (i,j,k = 1,\ldots,m-1) \tag{23}$$

- To account for the practical situation of multiple member buckling, the cross-terms between bifurcation modes and the limit-point mode satisfy:

$$V_{ijm} \neq 0 \quad (i,j = 1,\ldots,m-1; i \neq j) \tag{24}$$

$$V_{imm} = 0 \quad (i = 1,\ldots,m-1) \tag{25}$$

- The term for the the limit point enjoys:

$$V_{mmm} \neq 0 \tag{26}$$

On the basis of (12), (13), (18) and the assumptions (25) and (26), it suffices to consider the following third-order system of the total potential energy:

$$V = \frac{1}{2}\sum_{i=1}^{m-1}\sum_{j=1}^{m-1} V_{ijm} q_i q_j q_m + \frac{1}{6} V_{mmm} q_m^3 + \sum_{i=1}^{m} \dot{V}_i q_i \varepsilon + V'_m q_m \lambda \tag{27}$$

Differentiating V with respect to q_i $(i = 1,\ldots,m-1)$ and q_m leads to

$$\sum_{j=1}^{m-1} V_{ijm} q_j q_m + \dot{V}_i \varepsilon = 0 \quad (i = 1,\ldots,m-1) \tag{28}$$

$$\frac{1}{2}\sum_{i=1}^{m-1}\sum_{j=1}^{m-1} V_{ijm} q_i q_j + \frac{1}{2} V_{mmm} q_m^2 + \dot{V}_m \varepsilon + V'_m \lambda = 0 \tag{29}$$

It is natural to consider an imperfection in the direction involving all the active coordinates. However, we have to investigate a special imperfection in the direction of one of the active coordinates to verify the following scaling process by q_m. If $\dot{V}_i \neq 0$ for some $i = 1,\ldots,m-1$, $q_m \neq 0$ can be derived from (28). If $\dot{V}_i = 0$ for $i = 1,\ldots,m-1$ and $\dot{V}_m \neq 0$, (29) is generally satisfied by $q_m \neq 0$. Therefore, we can assume $q_m \neq 0$ in the sequel without loss of generality.

By dividing (28) by q_m, we can derive

$$\sum_{j=1}^{m-1} V_{ijm} q_j + \dot{V}_i \frac{\varepsilon}{q_m} = 0 \quad (i = 1,\ldots,m-1) \tag{30}$$

which is to be interpreted as a set of simultaneous linear equations of q_j $(j = 1,\ldots,m-1)$. Since $V_{iim} \neq 0$ $(i = 1,\ldots,m-1)$ are satisfied as the bifurcations are not degenerate (Ohsaki, 2001), q_j can be successfully found by solving (30) as

$$q_j = \tilde{q}_j \frac{\varepsilon}{q_m} \quad (j = 1,\ldots,m-1) \tag{31}$$

for a set of constants $\tilde{q}_j$ $(j = 1,\ldots,m-1)$. Then (30) is rewritten as

$$\sum_{j=1}^{m-1} V_{ijm}\tilde{q}_j + \dot{V}_i = 0 \quad (i = 1, \ldots, m-1) \tag{32}$$

With the use of (31) and (29) becomes

$$\left(\frac{1}{2}\sum_{i=1}^{m-1}\sum_{j=1}^{m-1} V_{ijm}\tilde{q}_i\tilde{q}_j\right)\frac{\varepsilon^2}{q_m^2} + \frac{1}{2}V_{mmm}q_m^2 + \dot{V}_m\varepsilon + V'_m\lambda = 0 \tag{33}$$

For each specified value of ε and $\tilde{q}_i (i = 1, \ldots, m-1)$, the independent variables in (33) are considered to be q_m and λ.

The condition for the critical point is written as

$$\frac{\partial\lambda}{\partial q_m} = 0 \tag{34}$$

By differentiating (33) with respect to q_m and by using (34), we can obtain the following equation:

$$-\left(\sum_{i=1}^{m-1}\sum_{j=1}^{m-1} V_{ijm}\tilde{q}_i\tilde{q}_j\right)\frac{\varepsilon^2}{q_m^3} + V_{mmm}q_m = 0 \tag{35}$$

Eq. (35) is solved as

$$q_m^2 = \sqrt{\frac{C_m}{V_{mmm}}}|\varepsilon| \tag{36}$$

where

$$C_m = \sum_{i=1}^{m-1}\sum_{j=1}^{m-1} V_{ijm}\tilde{q}_i\tilde{q}_j \tag{37}$$

By incorporating (36) into (33), we can obtain an imperfection sensitivity law

$$\lambda = -\frac{\dot{V}_m}{V'_m}\varepsilon - \frac{1}{V'_m}\sqrt{V_{mmm}C_m}|\varepsilon| \tag{38}$$

in which C_m is a function of $\tilde{q}_i$ and $\tilde{q}_j$ by (37) and, in general, cannot be expressed explicitly.

If there exist two symmetric bifurcation points at the limit point; i.e. $m = 3$, and $V_{12m} = 0$,

$$\tilde{q}_j = -\frac{\dot{V}_j}{V_{jjm}} \quad (j = 1, 2) \tag{39}$$

is obtained from (32). Therefore, (37) is expressed explicitly and, in turn, (38) reduces to

$$\lambda = -\frac{\dot{V}_3}{V'_3}\varepsilon - \frac{1}{V'_3}\sqrt{V_{333}\left(\frac{\dot{V}_1^2}{V_{113}} + \frac{\dot{V}_2^2}{V_{223}}\right)}|\varepsilon| \tag{40}$$

which agrees with the existing result (Thompson, 1982; Ikeda et al., 2005).

A fold line has come to be employed as an alternative means to deal with imperfection sensitivity (see, e.g., Eriksson et al., 1999; Lopez and Otranto, 2004). However, general properties of imperfection sensitivity can be obtained by the perturbation approach presented in this paper.

5. Numerical examples

Consider an arch-type truss as shown in Fig. 10, where $L = 250$, $H = 200$. A load ΛP is applied in vertical direction at the center node. The details of the analysis procedure are the same as those for the two-bar

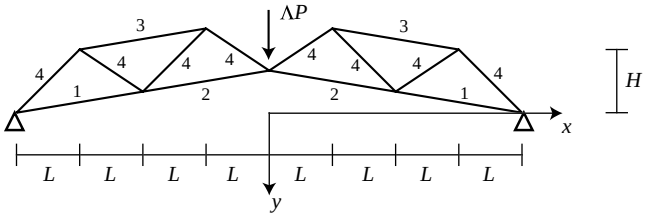

Fig. 10. An arch-type truss.

truss in Section 2. The elastic modulus E is 1 for simplicity, and $P = 0.001$. The members are divided into four groups as shown in Fig. 10. Let A_i and I_i, respectively, denote the cross-sectional area and second moment of area of the members in the ith group. The relation between I_i and A_i is assumed as

$$I_i = h_i^2 A_i \tag{41}$$

where h_i is independent of A_i.

Fig. 11 shows the relation between Λ and the vertical displacement v of the center node for the perfect system with $(A_1, A_2, A_3, A_4) = (100, 100, 1000, 300)$ and $(h_1, h_2, h_3, h_4) = (18.15, 18.05, 30.0, 100.0)$. A limit point is attained at $\Lambda = 4.7681$ as Λ is increased from 0.

Fig. 12 shows the variation of the five lowest eigenvalues e_i $(i = 1, \ldots, 5)$ with respect to v. Note that e_1 and e_2 are exactly coincident, and e_3 and e_4 are nearly coincident. The mode $\hat{\boldsymbol{p}}_5$ corresponds to the limit-point mode. The five eigenvalues vanish simultaneously at the hill-top point.

The eigenmodes $\hat{\boldsymbol{p}}_1, \ldots, \hat{\boldsymbol{p}}_5$ are as shown in Fig. 13. Since a set of modes that are orthogonal with respect to the Hessian of V is found by eigenvalue analysis, (25) is not usually satisfied. For example, $\hat{\boldsymbol{p}}_3$ and $\hat{\boldsymbol{p}}_4$ in Fig. 13 are symmetric with respect to the y-axis, and nodal displacements should exist to satisfy orthogonality with the limit-point mode $\hat{\boldsymbol{p}}_5$, which is also symmetric. Hence $\hat{\boldsymbol{p}}_3$ and $\hat{\boldsymbol{p}}_4$ are the mixture of the limit-point mode and the member buckling mode. V_{333} does not vanish since $\hat{\boldsymbol{p}}_3$ and $-\hat{\boldsymbol{p}}_3$ correspond to different physical behaviors; V_{444} also does not vanish. Note that $\hat{\boldsymbol{p}}_1$ and $\hat{\boldsymbol{p}}_2$ are antisymmetric with respect to the y-axis, and vertical displacements of the center node vanish; therefore, $V_{111} = V_{222} = 0$ is satisfied.

In order to distinguish limit-point mode and member buckling modes, the limit-point mode $\hat{\boldsymbol{p}}_5$ is first defined as the increment of displacements at the limit point while tracing the equilibrium path by the displacement increment method. The components of $\hat{\boldsymbol{p}}_5$ are subtracted from $\hat{\boldsymbol{p}}_3$ and $\hat{\boldsymbol{p}}_4$ to arrive at pure member

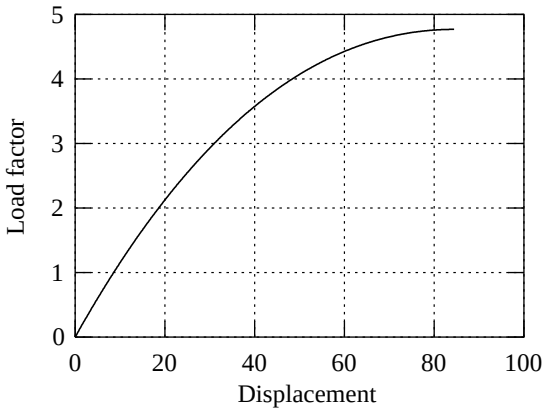

Fig. 11. Relation between load factor and vertical displacement of the center node.

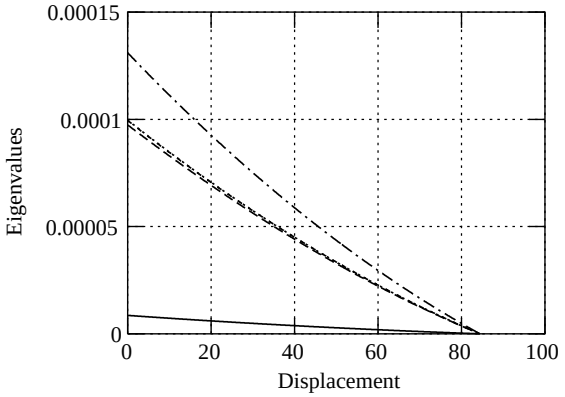

Fig. 12. Relation between eigenvalues and vertical displacement of the center node.

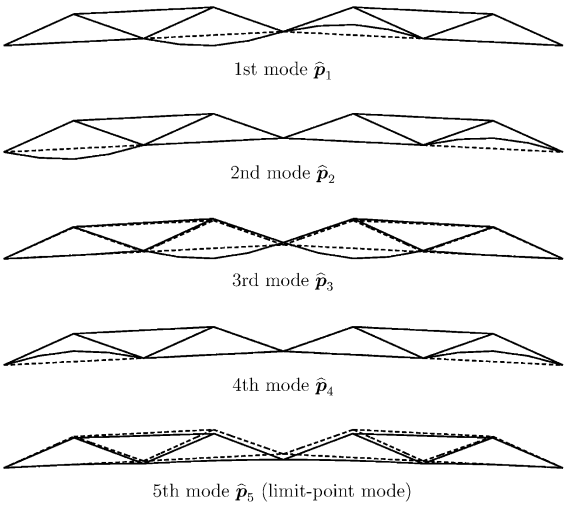

Fig. 13. Eigenmodes corresponding to the five zero eigenvalues satisfying orthogonality condition.

buckling modes $\boldsymbol{p}_3$ and $\boldsymbol{p}_4$ shown in Fig. 14. Note that symmetric modes $\boldsymbol{p}_3$, $\boldsymbol{p}_4$ and $\boldsymbol{p}_5$ do not satisfy the orthogonality condition.

The third differential coefficients of V are obtained as

$$\begin{aligned} &V_{115} = V_{335} = -2.0842 \times 10^{-7}, \quad V_{225} = V_{445} = -2.1415 \times 10^{-7}, \\ &V_{345} = -2.2262 \times 10^{-9}, \quad V_{555} = -1.8214 \times 10^{-8} \end{aligned} \tag{42}$$

It has been confirmed that the absolute values of the coefficients that are assumed to vanish in (23) and (25) are nonzero but are small enough compared with those in (42). Other coefficients are

$$\begin{aligned} &\dot{V}_1 = \dot{V}_2 = -9.7979 \times 10^{-5}, \quad \dot{V}_3 = \dot{V}_4 = -9.7963 \times 10^{-5}, \\ &\dot{V}_5 = -4.7352 \times 10^{-5}, \quad V'_5 = -7.0748 \times 10^{-11} \end{aligned} \tag{43}$$

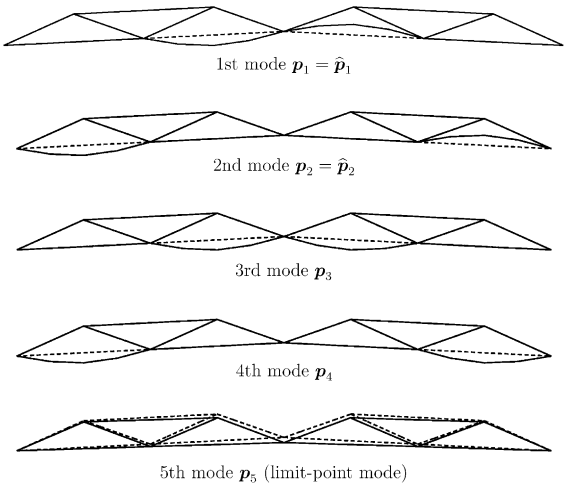

Fig. 14. Eigenmodes corresponding to the five zero eigenvalues satisfying $V_{iii} = 0$ ($i = 1, 2, 3, 4$).

First consider an imperfection in the direction of the sum $\varepsilon\sum_{i=1}^{5}\boldsymbol{p}_i$ of five modes shown in Fig. 14. The use of (42) and (43) in 38 leads to

$$\lambda = -1.8393 \times 10^{-2}\varepsilon - 0.22176|\varepsilon| \tag{44}$$

The relation between λ and ε is plotted in Fig. 15, where '+' mark is the maximum load factor of an imperfect system obtained by nonlinear path-following analysis, and the solid line is the piecewise linear estimation by (44). Note that the maximum load factor of an imperfect system is attained at a limit point. It is observed from Fig. 15 that the maximum load factors of imperfect systems can be estimated with good accuracy by the linear sensitivity relation (44). Note that each member is divided into four elements, and the initial imperfection is given as a piecewise linear shape for path-following analysis of an imperfect system. On the other hand, a curved shape is assumed in computing $\dot{V}_i$. However, it has been ensured from the numerical results that discretizing errors due to the modeling stated above are negligible.

For the imperfection $\varepsilon\boldsymbol{p}_5$ in the direction of limit-point mode, the second term in the right-hand side of (44) vanishes, and the relation between λ and ε is given by a linear law

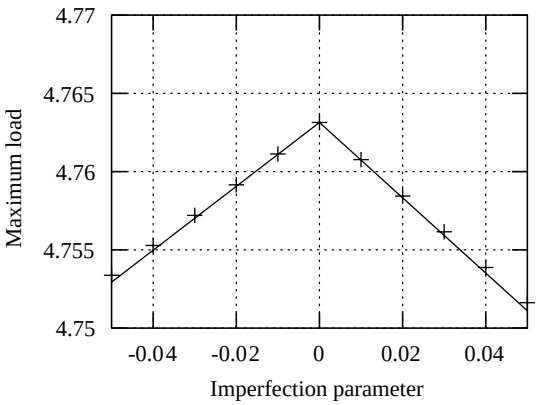

Fig. 15. Relation between maximum load and imperfection parameter that includes five modes.

$$\lambda = -1.8393 \times 10^{-2}\varepsilon \tag{45}$$

which is plotted in Fig. 16.

For the imperfection $\varepsilon \boldsymbol{p}_1$, the first term in the right-hand side of (44) vanishes, and the relation between λ and ε is given by a piecewise linear law

$$\lambda = -0.11134|\varepsilon| \tag{46}$$

which is plotted in Fig. 17. For the third mode $\varepsilon \boldsymbol{p}_3$, the relation is

$$\lambda = -0.11249|\varepsilon| \tag{47}$$

which is plotted in Fig. 18. Note that although the mode $\varepsilon \boldsymbol{p}_3$ corresponds to a slightly asymmetric bifurcation, the linear term ε is negligibly small.

The maximum loads have thus been accurately estimated by linear and piecewise linear relations for all the cases to assess the validity of the proposed formula (44).

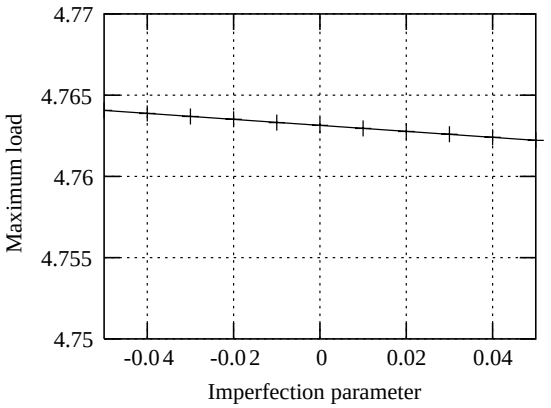

Fig. 16. Relation between maximum load and imperfection parameter for $\varepsilon \boldsymbol{p}_5$ (limit-point mode).

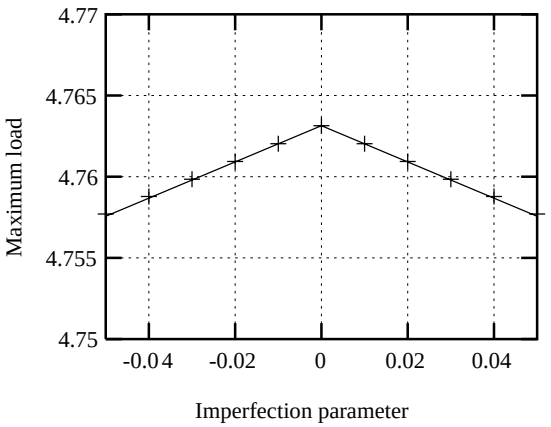

Fig. 17. Relation between maximum load and imperfection parameter for $\varepsilon \boldsymbol{p}_1$.

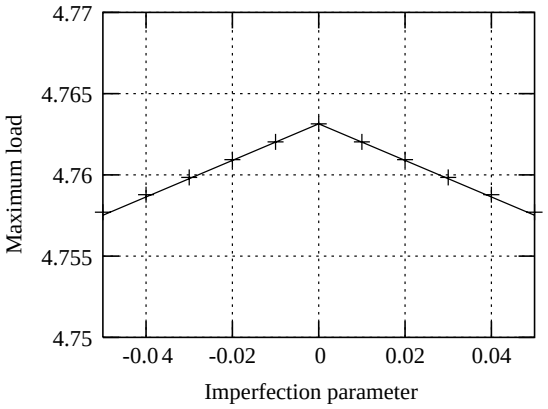

Fig. 18. Relation between maximum loads and imperfection parameter for $\varepsilon \boldsymbol{p}_2$.

6. Conclusions

Imperfection sensitivity formulas have been developed for a hill-top branching point that has many symmetric bifurcation points at the limit point. The problem considered here is practically very important for estimating the imperfection sensitivity of interaction of global snapthrough and local member buckling. The maximum loads of imperfect systems are piecewise linear functions of imperfection parameter. Therefore, the existence of member buckling at the limit point is not dangerous in view of imperfection sensitivity. The "simultaneous mode design" for this case is not that pessimistic as was cautioned the "erosion of optimization by compound bifurcation."

References

Eriksson, A., Pacoste, C., Zdunek, A., 1999. Numerical analysis of complex instability behavior using incremental-iterative strategies. Computer Methods for Applied Mechanics and Engineering 179, 265–305.

Godoy, L.A., 1999. Theory of Elastic Stability: Analysis and Sensibility. Taylor & Francis.

Hunt, G.W., 1981. An algorithm for the nonlinear analysis of compound bifurcation. Philosophical Transactions of the Royal Society of London Series A 300, 443–471.

Hunt, G.W., 1986. Hidden (a)symmetries of elastic and plastic bifurcation. Applied Mechanics Reviews 39 (8), 1165–1186.

Hutchinson, J.W., Amazigo, C., 1967. Imperfection-sensitivity of eccentrically stiffened cylindrical shells. AIAA Journal 5 (3), 392–401.

Ikeda, K., Ohsaki, M., Kanno, Y., 2005. Imperfection sensitivity of hilltop branching points of systems with dihedral group symmetry. International Journal of Non-Linear Mechanics 40, 755–774.

Ikeda, K., Oide, K., Terada, K., 2002. Imperfection sensitive variation of critical loads at hilltop bifurcation point. International Journal of Engineering Science 40, 743–772.

Koiter, W.T., Kuiken, G.D.C., 1971. The interaction between local buckling and overall buckling in the behavior of built-up columns. Report WTHD-23, Delft University of Technology, Delft, Holland.

Lopez, S., Otranto, E., 2004. Evaluation of the fold line by asymptotic extrapolation for structural analysis. International Journal of Structural Stability and Dynamics 4-2, 147–170.

Needleman, A., 1972. A numerical study of necking in circular cylindrical bars. Journal of the Mechanics and Physics of Solids 20 (2), 111–127.

Ohsaki, M., 2000. Optimization of geometrically nonlinear symmetric systems with coincident critical points. International Journal of Numerical Methods in Engineering 48, 1345–1357.

Ohsaki, M., 2001. Sensitivity analysis and optimization corresponding to a degenerate critical point. International Journal of Solids and Structures 38, 4955–4967.

Ohsaki, M., 2003. Sensitivity analysis of an optimized bar-spring model with hill-top branching. Archives of Applied Mechanics 73, 241–251.

Okazawa, S., Oide, K., Ikeda, K., Terada, K., 2002. Imperfection sensitivity and probabilistic variation of tensile strength of steel members. International Journal of Solids and Structures 39 (6), 1651–1671.

Peek, R., Triantafyllidis, N., 1992. Worst shapes of imperfections for space trusses with many simultaneously buckling modes. International Journal of Solids and Structures 29 (19), 2385–2402.

Spunt, L., 1971. Optimum Structural Design. Prentice-Hall, Englewood Cliffs.

Supple, W.J., 1967. Coupled branching configurations in the elastic buckling of symmetric structural system. International Journal of Mechanical Science 9, 97–112.

Supple, W.J., 1968. On the change in buckle pattern in elastic structures. International Journal of Mechanical Science 10, 737–745.

Thompson, J.M.T., 1982. Instabilities and Catastrophes in Science and Engineering. John Wiley, Chichester.

Thompson, J.M.T., Hunt, G.W., 1973. A General Theory of Elastic Stability. John Wiley, New York.

Thompson, J.M.T., Hunt, G.W., 1974. Dangers of structural optimization. Engineering Optimization 1, 99–110.

Thompson, J.M.T., Hunt, G.W., 1984. Elastic Instability Phenomena. John Wiley, Chichester.

Thompson, J.M.T., Lewis, G.M., 1972. On the optimum design of thin-walled compression members. Journal of the Mechanics and Physics of Solids 20 (2), 101–109.

Thompson, J.M.T., Schorrock, P.A., 1975. Bifurcation instability of an atomic lattice. Journal of the Mechanics and Physics of Solids 23 (1), 21–37.

Thompson, J.M.T., Supple, W.J, 1973. Erosion of optimum designs by compound branching phenomena. Journal of the Mechanics and Physics of Solids 21 (3), 135–144.

Tvergaard, V., 1973. Imperfection-sensitivity of a wide integrally stiffened panel under compression. International Journal of Solids and Structures 9 (1), 177–192.